Plant Physiology and Biochemistry 139 (2019) 141–151

Contents lists available at ScienceDirect

Plant Physiology and Biochemistry

journal homepage: www.elsevier.com/locate/plaphy

Research article

Identification of leucoanthocyanidin reductase and anthocyanidin reductase genes involved in proanthocyanidin biosynthesis in *Malus* crabapple plants

Hua Li[a,b,c,1], Ji Tian[a,b,c,1], Yu-yan Yao[a,b,c,1], Jie Zhang[a,b,c], Ting-ting Song[a,b,c], Ke-ting Li[a,b,c], Yun-cong Yao[a,b,c,*]

[a] Beijing Advanced Innovation Center for Tree Breeding by Molecular Design, Beijing University of Agriculture, Beijing, China
[b] Plant Science and Technology College, Beijing University of Agriculture, Beijing, China
[c] Beijing Collaborative Innovation Center for Eco-environmental Improvement with Forestry and Fruit Trees, Beijing, China

ARTICLE INFO

Keywords:
Proanthocyanins
Anthocyanins
Flavonols
Malus crabapple

ABSTRACT

Proanthocyanidins (PAs) from plants are a nutritionally valuable component of the human diet and play important roles in defense against pests and diseases. PAs are products of the flavonoid pathway, which also leads to the production of anthocyanins and flavonols. The enzymes leucoanthocyanidin reductase (LAR) and anthocyanidin reductase (ANR) are involved in PA biosynthesis. The PA biosynthetic pathway has been characterized in several plant species, but the relationship between its expression and PA accumulation in *Malus* crabapple remains unclear. Here, we cloned the LAR genes *MrLAR1*, *2*, and the ANR genes *MrANR1*, *2*, from the red leaved *Malus* crabapple cultivar 'Royalty'. The contents of PAs and the expression levels of the *LAR* and *ANR* genes were investigated in different organs of the two crabapple cultivars. The transcript levels of two *LAR* genes and two *ANR* genes correlated with the contents of the catechin and epicatechin, which are proanthocyanidin precursors. Over-expression of the *MrLAR1*, *2* and *MrANR1*, *2* in tobacco (*Nicotiana tabacum*) promoted the accumulation of PAs, while transient silencing of their expression in crabapple resulted in reduced PA levels. In addition, a negative correlation between quercetin, anthocyanin, and PA biosynthesis was also found during crabapple leaf and fruit peel development. We also found that *MrLAR1* and *2* may contribute to epicatechin biosynthesis. In summary, the *LAR* and *ANR* genes are critical factors in PA biosynthesis, and there is competition between the quercetin, anthocyanin, and PA biosynthetic pathways during leaf and fruit peel development in *Malus* crabapple.

1. Introduction

Flavonoids are a diverse group of plant secondary metabolites with biological functions, which include proanthocyanins (PAs), anthocyanins, and flavonols as the main products of the biosynthetic pathway. The main known functions of PAs, also called condensed tannins, are to provide protection, through multiple mechanisms, against microbial pathogens, as well as insects and herbivores (Dixon et al., 2005; Santos-Buelga and Scalbert, 2000). PAs also act as dietary antioxidants with beneficial effects on human health, including reducing free radical-mediated injury and cardiovascular disease (Middleton et al., 2000).

PAs are phenolic polymers that are formed by the condensation of flavan-3-ol monomeric units, such as catechin and epicatechin. PA biosynthesis shares common steps with flavonols and anthocyanins, and their branch point is at the biosynthesis of leucoanthocyanidin. Leucoanthocyanidin reductase (LAR) and anthocyanidin reductase (ANR) catalyze the final reactions in the PA biosynthetic pathway, LAR converts leucoanthocyanidin (flavan-3,4-diols) to catechin, whereas ANR catalyzes the synthesis of epicatechin from anthocyanidin (Tanner et al., 2003).

The PA biosynthetic pathway has been characterized in several plant species, including Arabidopsis (*Arabidopsis thaliana*), grapes (*Vitis vinifera*), and apple (*Malus domestica*). In *Arabidopsis* lacking a functional *LAR* gene, PA synthesis exclusively produces epicatechin (2,3-cis-flavan-3-ol), which is synthesized by ANR (encoded by the *BANYULS* gene) from anthocyanidins only in the seed coat (Dixon et al., 2005; Xie et al., 2003). In grape, both LAR and ANR are activated early and synthesized during flowering and berry development, facilitating precocious tannin biosynthesis (Gagné et al., 2009). Recently, several studies have focused on the expression of PA biosynthetic genes in

* Corresponding author. Beijing Collaborative Innovation Center for Eco-environmental Improvement with Forestry and Fruit Trees, Beijing 102206, China.
E-mail address: yaoyc_20@126.com (Y.-c. Yao).
[1] Contributed equally to this work.

https://doi.org/10.1016/j.plaphy.2019.03.003
Received 27 December 2018; Received in revised form 18 February 2019; Accepted 4 March 2019
Available online 08 March 2019
0981-9428/

apple, where catechin and epicatechin biosynthesis have been found to be under the control of the *MdLAR1* and *MdANR* biosynthetic genes, respectively (Henrykirk et al., 2012; Liao et al., 2015). Transformation experiments have further demonstrated the function of *ANR* in plants as over-expressing the *ANR* genes from Medicago (*Medicago truncatula*) in tobacco resulted in increased levels of PAs (Xie et al., 2003, 2004). Suppression of the PA branch point genes, *ANR1* and g*ANR2*, have also been shown to result in reduced PA levels and an over-accumulation of specific anthocyanins in the seed coat of soybean (*Glycine max*) (Kovinich et al., 2012).

The flavonoid pathway also produces anthocyanins and flavonols. One of the most common anthocyanin pigments are cyanidin-based anthocyanins (cyanidin-3-galactoside), which are the main coloration pigment in *Malus* crabapple leaves (Tian et al., 2015). The synthesis of PAs and anthocyanins share common steps in the flavonoid pathway, leading to the synthesis of flavan-3,4-diols (Tian et al., 2015), and it has been proposed that there is competition between the PA and anthocyanin biosynthetic pathways (Verdier et al., 2012). In purple-leaf tea (*Camellia sinensis* L.), anthocyanins and flavonols accumulate to remarkably high levels in leaves, while the total amount of catechins is low (He et al., 2018). However, the function of *LAR* and *ANR,* and the competition between quercetin, anthocyanin, and PA biosynthesis has not yet been determined in many species, such as *Malus* spp. 'Royalty' and *Malus* spp. 'Flame'.

Malus crabapple plays an important role in ornamental and economically important germplasm collection, which acts as a valuable model organism to study the biosynthetic mechanism of flavonoid formation, due to its considerable color diversity and notably high resistance to abiotic stress (Tian et al., 2011). Furthermore, the leaves and fruits of crabapple are rich in flavonoid compounds and can serve as food nutrition additives that provide an excellent source of antioxidants (Martin, 2013).

In this study, we investigated the role of the *LAR* genes and *ANR* genes in the PA biosynthesis pathway in crabapple leaves and fruits. Their expression profiles were examined in two crabapple cultivars and in different tissues during late development. The relationship between the expression levels of *LAR* and *ANR* genes and PA content was also determined. To verify the proposed biochemical activity of the two genes, we over-expressed and silenced them in tobacco and crabapple plants, respectively. Their role in PA biosynthesis, and the association with the biosynthesis of anthocyanin and quercetin synthesis during the late development of leaves and fruit peels, is discussed.

2. Materials and methods

2.1. Plant material

Two crabapple (*Malus* spp.) cultivars were used in this study: (i) *Malus* spp. 'Royalty', a red leaved cultivar; and (ii) *Malus* spp. 'Flame', a green leaved cultivar. Eight-year-old trees were grafted onto *Malus hupehensis* and planted at the Crabapple Germplasm Resources Nursery, at the Beijing University of Agriculture (40.1°N, 116.6°E). Three trees of each cultivar showing similar growth were used, and leaf samples were collected from shoots in the southeastern part of the tree canopy. The leaves of 'Royalty' and 'Flame' were collected at 42, 49, 56, 63, and 70 days after budbreak (S1-S5, 'S' represent 'stage'). The fruit peels were collected at 60, 80, and 100 days after full bloom (S1, S2, S3, 'S' represent 'stage'). In RNA-seq, the leaves of 'Royalty' and 'Flame' were collected at 14 days and 42 days after budbreak (young stage and mature stage), the fruit peels were collected at 20 days and 60 days after full bloom (young stage and mature stage). All of the leaves and fruits selected were phenotypically similar for each stage (i.e., shape, size and color) and harvested at the same time (morning) of the day. All of the leaves were frozen in liquid nitrogen upon collection, and stored at −80 °C prior to HPLC analysis or RNA extraction. The peel of each fruit was pared to a thickness of approximately 1 mm, frozen immediately in liquid nitrogen, and then stored at −80 °C prior to HPLC analysis or RNA extraction.

Nicotiana benthamiana plants were maintained in a greenhouse (20–22 °C, 16 h light; relative humidity, 60%) of the Fruit Tree Key Laboratory at the Beijing University of Agriculture and 5- to 7-week-old plants (young plant grown up to six leaves and a smallest leaf length greater than 1 cm) were used for agroinfiltration.

'Royalty' tissue culture plants were established from one-year-old wood before spring bud germination, cultured on Murashige and Skoog medium supplemented with 0.1 mg/L 6-Benzylaminopurine (6-BA) and 2 mg/L (2, 4-dichlorophenoxy) acetic acid (2,4-D) at 22 °C for a 16-h light (200 μmol s^{-1} m^{-2})/8-h dark period for 30 d to induce leaf reproduction before collection.

2.2. RNA quantification and quality analysis

RNA degradation and contamination were visualized on 1% agarose gels. RNA purity was confirmed using the Nano Photometer® spectrophotometer (IMPLEN). RNA concentration was measured using the Qubit® RNA Assay Kit in a Qubit® 2.0 Fluorometer (Life Technologies). RNA integrity was assessed using the RNA Nano 6000 Assay Kit from the Bioanalyzer 2100 system (Agilent Technologies).

2.3. RNA-seq library preparation

A 3 μg aliquot of RNA per sample was used as input material for each of the RNA sample preparations. Sequencing libraries were generated using the NEBNext® Ultra™ RNA Library Prep Kit for Illumina® (NEB) following the manufacturer's recommendations, and index codes were added to label each sample. In order to preferentially select cDNA fragments 150–200 bp in length, the library fragments were purified with the AMPure XP system (Beckman Coulter). Then 3 ml of USER Enzyme (NEB) was used with size-selected, adaptor-ligated cDNA at 37 °C for 15 min followed by 5 min at 95 °C. PCR was performed with the Phusion High-Fidelity DNA polymerase, Universal PCR primers and Index (X) Primers. Finally, PCR products were purified (AMPure XP system) and library quality was assessed using the Agilent Bioanalyzer 2100 system.

2.4. Read mapping to the reference genome and quantification of gene expression

An index of the reference genome was built using Bowtie v2.2.3 (Langmead et al., 2009), and paired-end clean reads were aligned to the apple reference genome (Velasco et al., 2010) using TopHat v2.0.12 (Trapnell et al., 2009). HTSeq v0.6.1 (https://pypi.python.org/pypi/HTSeq) was used to count the read numbers mapped to each gene (Anders et al., 2015). The RPKM (Reads Per Kilo bases per Million mapped Reads) method was used to investigate differential gene expression at different developmental stages of leaves and fruits, and the RPKM of each gene was calculated based on the length of the gene and read counts mapped to this gene (Mortazavi et al., 2008).

2.5. Differential expression analysis

Differential expression analysis of four groups (three biological replicates per group) was performed using the DESeq R package (1.18.0) (http://www.biocon-ductor.org/packages/release/bioc/html/DESeq.html). DESeq provides statistical routines for determining differential expression in 50 digital gene expression data using a model based on the negative binomial distribution. The resulting *P*-values were adjusted using the Benjamini and Hochberg approach for controlling the false discovery rate (Benjamini and Hochberg, 1995). Genes with an adjusted *P*-value < 0.05 found by DESeq were considered to be differentially expressed (Anders and Huber, 2010).

2.6. High pressure liquid chromatography (HPLC) analysis

For flavonoid extraction, 1.0 g of frozen crabapple leaves, crabapple fruit peels, and tobacco leaves were powdered in liquid nitrogen using a mortar and pestle. Then, 3 ml of methanol/water/formic acid (80:19:1, v/v/v) was added to the sample, followed by 50 min of sonication at 12,000 Hz at 45 °C to extract the flavonoid compounds. The compounds were filtered through a 0.22 μm membrane (Shanghai ANPEL, Shanghai, China) before HPLC analyses. We used mixed leaf samples from S1 to S5 and fruit peel samples from S1 to S3 for the identification of flavonoid types and for the detection of temporal changes in the leaf and fruit peel flavonoid composition during leaf and fruit peel development.

Experimental standards of cyanidin-3-O-galactoside, quercetin-3-O-glucoside and quercetin-7-O-rhamnoside were purchased from Sigma-Aldrich (Steinheim, Germany); experimental standards of procyanidin B2, (−)-epicatechin, and catechin were purchased from Sigma-Aldrich (Poole, U.K.); data obtained for experimental standards and information regarding the identified compounds were combined to identify the flavonoids.

An Agilent 1100 series HPLC system (Agilent Technologies, Wilmington, DE, USA) was used in our experiments. For chromatographic separation, eluent A was 0.5% aqueous formic acid, eluent B was 100% acetonitrile, and the elution gradient was as follows: 90% A at 0min, 90% A to 81% A from 0 to 40min, 81% A to 60% A from 40 to 50 min, 90% A at 50.01 min, and 90% A at 60 min. The flow rate was 1.0 ml/min, and injection volume was 20 μl. The ZORBAX Eclipse XDB-C18 (5 μm, 150 × 4.6 mm, Agilent, USA) analytical column temperature was 27 °C for all analyses. Chromatograms were acquired at 520 nm for anthocyanins and at 350 and 280 nm for all other flavonoids. DAD data were recorded from 200 to 600 nm.

2.7. Cloning and sequence analysis of full-length MrLAR and MrANR genes

Total RNA was extracted from crabapple leaves using an RNA Extraction Kit (Aidlab, Beijing, China) according to the manufacturer's instructions. Based on the *MdLAR* sequences (GenBank Accession Number AFZ93013.1 and AFZ93011.1) and the *MdANR* sequences (GenBank Accession Number JN035299 and AF117269) in the NCBI database, a pair of oligo nucleotide primers (Table S1) were designed to isolate the corresponding *MrLAR* and *MrANR* cDNA sequences (for cDNA synthesis see below). PCR reaction conditions were 95 °C, 5 min followed by 35 cycles of 30 s at 94 °C, 30 s at 60 °C, and 90 s at 72 °C. All PCR products were sub-cloned into the pGEM T-Easy Vector (Promega, Madison, WI) and transformed into *Escherichia coli* DH5α cells and sequenced. Comparison and analysis of the sequences was performed using the advanced BLAST software at the National Center for Biotechnology Information (http://www.ncbi.nlm.nih.gov). The full-length DNA and protein sequences were aligned using DNAMAN 5.2.2 (Lynnon Biosoft, USA). Phylogenetic and molecular evolutionary analyses were conducted with MEGA version 5.1, using a minimum evolution phylogeny test with 1000 bootstrap replicates (Kumar et al., 2004).

2.8. Quantitative real-time PCR analysis

Total RNA from crabapple leaves and fruit peels was extracted as described above. DNase I (TaKaRa, Ohtsu, Japan) was added to remove genomic DNA, and the samples were then subjected to cDNA synthesis using the Access RT-PCR System (Promega, USA), according to the manufacturer's instructions. The expression levels of flavonoid biosynthetic genes in crabapple and tobacco were analyzed using quantitative real-time PCR (RT-qPCR), the SYBR Green qPCR Mix (TaKaRa, Ohtsu, Japan) and the Bio-Rad CFX96 Real-Time PCR System (BIO-RAD, USA), according to the manufacturers' instructions. The PCR primers were designed using NCBI Primer BLAST (https://www.ncbi.nlm.nih.gov/tools/primer-blast/) and are listed in Table S1.

RT-qPCR analysis was carried out in a total volume of 20 μl containing 9 μl of 2 × SYBR Green qPCR Mix (TaKaRa, Ohtsu, Japan), 0.1 μM specific primers (each), and 100 ng of template cDNA. The reaction mixtures were heated to 95 °C for 30 s, followed by 39 cycles at 95 °C for 10 s, 50–59 °C for 15 s, and 72 °C for 30 s. A melting curve was generated for each sample at the end of each run to ensure the purity of the amplified products. The expression levels and correlation of flavonoid regulatory and biosynthetic genes were calculated using CFX-Manager-3-1 following the manufacturer's instructions (Bio-Rad). The transcript levels were normalized to the expression of the *Malus 18S ribosomal RNA* gene (DQ341382, for apple and crabapple) and the *NtActin* gene (GQ339768, for tobacco) as the internal controls (Livak and Schmittgen, 2001).

2.9. Transient overexpression in tobacco leaves

The full length *MrLAR1*, *2* and *MrANR1*, *2* open reading frame (ORF) sequences were cloned into the pBI121 vector using the *Bam*HI and *Sac*I sites, and *Agrobacterium tumefaciens* strains GV3101 carrying these constructs were used to transiently transform tobacco leaves (Jefferson et al., 1987). *N. benthamiana* infiltration was performed as previously described (Tian et al., 2017). The primers used are listed in Table S1.

2.10. Transient expression assays in crabapple leaves

Fragments for the pTRV2-*MrLAR1* (1,065bp), pTRV2-*MrLAR2* (1,050bp) and pTRV2-*MrANR1* (1,020bp), and pTRV2-*MrANR2* (1,020bp) constructs were amplified by PCR, using gene-specific primers, from a cDNA library derived from *Malus* crabapple leaves (spp. 'Royalty') using Taq DNA polymerase (TaKaRa, Ohtsu, Japan) according to the manufacturer' s instructions. The PCR primers used are shown in Table S1.

A. tumefaciens cells were grown, collected, and resuspended in a 10 mM MES (pH 5.6), 10 mM $MgCl_2$, and 200 mM acetosyringone solution to a final optical density of 1.5 at 600 nm, and then incubated at room temperature for 3–4 h without shaking. Before infiltration, *A. tumefaciens* cultures containing pTRV1 and pTRV2, or its derivatives (pTRV2-*MrLAR1*, pTRV2-*MrLAR2* and pTRV2-*MrANR1*, pTRV2-*MrANR2*), were mixed in a 1:1 ratio (Tian et al., 2017). The infiltration protocol for transient expression assays in crabapple tissue culture plants was adapted as previously described (Tian, 2014). Treated plants were then cultured in MS medium (see above) in the dark for 12–16 h after washing with distilled water (with 50 mg/L kanamycin and 100 mg/L cefotaxime sodium added). 14 days post-infiltration, the infected leaves were collected to investigate phenotypic and gene expression differences.

2.11. Visualization of PAs using 4-dimethylaminocinnamaldehyde (DMACA)

The infiltrated tobacco leaves were used for visualization of PAs by DMACA staining. DMACA [0.1% (w/v)] stain was prepared in absolute ethanol containing 1% (w/v) hydrochloric acid (Chevalier et al., 2003). Leaf discs were excised from fully expanded leaves of tobacco and decolorized using an ethanol and glacial acetic acid mixture in a 3:1 ratio for 20 min. The de-colorized leaf discs were then immersed in fresh staining solution and incubated on a shaker for 4–5 h. Finally, the leaf discs were washed for 10 min with 70% ethanol and images were captured.

2.12. Statistical analysis

Significant differences among the experimental data were set to $P = 0.05$. The data were analyzed using a one-way ANOVA followed by

Duncan's and Tukey's multiple range tests in Microsoft Excel 2010 (Microsoft, USA) and IBM SPSS Statistics 20 (IBM, USA). The relationships between the data were analyzed using Pearson's test with IBM SPSS Statistics 20. Graphs were made with R, MEGA version 5.1, Interaction Tree Of Life (ITOL) (http://itol.embl.de/), DNAMAN, OriginPro 8.5 statistical software (OriginLab Corporation, United States), and Microsoft Office PowerPoint 2010.

3. Results

3.1. Bioinformatic analysis of leaf and fruit peel data

To determine the expression of genes involved in the PA metabolic pathway of the two crabapple cultivars, we selected two representative development stages of leaves and fruit peels of 'Royalty' and 'Flame' for RNA-seq.

Total RNA was extracted from three biological replicates of two different leaves and fruits developmental stages of 'Royalty' and 'Flame' plants and used to generate cDNA libraries. After removing reads derived from rRNA and those of low quality, the total length of clean reads ranged from 9,244,289 to 23,663,852 among the different libraries, and almost 66% of the sequenced reads could be aligned to the apple genome (Table 1). A pearson correlation analysis indicated that the sixteen libraries from the leaves and fruit peels of two developmental stages of *M*. 'Royatly' and *M*. 'Flame' had highly consistent transcriptome profiles (r^2 = 0.573–0.987; see Supplementary Fig. S1).

Reads Per Kilo bases per Million mapped reads' (RPKM) values were used to investigate transcript differences. As a result, 844 genes (ratio > 2.0, *P*-value < 0.05) were found to be up-regulated and 1007 genes (ratio > 2.0, *P*-value < 0.05) down-regulated in 'Royalty' mature leaf (Royalty_ML) vs. 'Royalty' young leaf (Royalty_YL); 1179 genes (ratio > 2.0, *P*-value < 0.05) were found to be up-regulated and 1423 genes (ratio > 2.0, *P*-value < 0.05) down-regulated in 'Royalty' mature fruit (Royalty_MF) vs. 'Royalty' young fruit (Royalty_YF); 833 genes (ratio > 2.0, *P*-value < 0.05) were found to be up-regulated and 984 genes (ratio > 2.0, *P*-value < 0.05) down-regulated in 'Flame' mature leaf (Flame_ML) vs. 'Flame' young leaf (Flame_YL); 1637 genes (ratio > 2.0, *P*-value < 0.05) were found to be up-regulated and 1107 genes (ratio > 2.0, *P*-value < 0.05) down-regulated in 'Flame' mature fruit (Flame_MF) vs. 'Flame' young fruit (Flame_YF) (Supplementary Fig. S2).

Clustering analysis of the expression patterns in PA metabolic pathway related genes at the young and mature stages of leaves and fruit peels both in 'Royalty' and 'Flame' are shown in Fig. 1A. Most of the PA metabolic pathway related genes showed a significant reduction in expression during the development of both leaf and fruit peel, although the expression of *MrFLS* (flavonol synthase, comp68350_c0) increased during maturation of the fruit peels in both cultivars. The same increasing trend was also observed for *MrLAR* (comp59267_c0) in 'Flame' fruit peels and for *MrF3H* (flavanone 3-hydroxylase, comp65910_c0) in 'Royalty' and 'Flame' fruit peels (Fig. 1A).

The 1,065bp *MrLAR1* and 1,050bp *MrLAR2* cDNA sequences are predicted to encode 335 and 350 amino acid protein sequences, respectively, and the 1020 bp full-length cDNAs of both *MrANR1* and *2* encoded 399 amino acid proteins. The MrLAR1 and 2 protein sequences showed 99% and 97.71% sequence identities with MdLAR1 and MdLAR2, and MrANR1 and 2 protein sequences showed 98.82% and 98.82% sequence homologies with MdANR1 and MdANR2, respectively, which are known PA biosynthetic proteins from apple (Fig. 1B and C). In addition, the RFLP, ICCN, and THD motifs are identical between MrLAR1 and MrLAR2 (Fig. 1B). A phylogenetic tree also showed that MrLAR and MdLAR, PcLAR had higher sequence similarity with each other than with homologs from other plants, and this was also true for MrANR and the MdANR, PcANR (Fig. 1D).

We also cloned the *ANR* and *LAR* genes from the green leaved *Malus* crabapple cultivar 'Flame, and named as *MfLAR1*, *MfLAR2* and *MfANR1*, *MfANR2* genes. Sequence alignment results showed that there were no significant sequence differences observed in *ANR* and *LAR* genes in these two cultivars (Supplemental Fig. S3).

3.2. Flavonoid concentrations and relative genes expression in leaves and fruit peels during late development

Due to the significant differences of flavonoids in both leaves and fruit peels during different developmental stages in crabapple, samples of leaves and fruit peels were collected during early and late development of 'Royalty' and 'Flame' (Fig. 2). In 'Royalty' leaves during late development, an increase in quercetin and anthocyanin levels were observed, alongside a decrease in PA, epicatechin, and catechin abundance (Fig. 2B). Similar trends were observed in 'Flame', except for the

Table 1
Summary of RNA-seq data from leaves and fruit peels of 'Royalty' and 'Flame'.

Sample	Raw reads	Clean reads	Clean bases	Error (%)	Q20 (%)	Q30 (%)	GC (%)
Royalty_ML_1	14,664,031	14,059,796	2.1G	0.03	97.68	92.46	48.77
Royalty_ML_2	15,743,754	15,044,853	2.26G	0.03	97.42	92.35	48.74
Royalty_ML_3	15,462,865	14,753,353	2.22G	0.03	97.58	92.43	48.66
Royalty_YL_1	12,713,799	12,069,762	1.83G	0.03	97.49	92.09	49.79
Royalty_YL_2	14,242,975	13,674,975	2.07G	0.03	97.24	91.74	49.72
Royalty_YL_3	11,643,753	11,035,647	1.66G	0.03	97.51	92.12	49.67
Royalty_MF_1	15,980,302	15,593,160	2.34G	0.03	97.72	92.49	47.92
Royalty_MF_2	14,643,785	14,376,564	2.16G	0.03	97.74	92.51	47.95
Royalty_MF_3	13,967,435	13,454,242	2.03G	0.03	97.56	92.23	47.59
Royalty_YF_1	16,849,706	15,797,378	2.39G	0.03	97.76	92.8	47.34
Royalty_YF_2	17,435,467	15,983,864	2.41G	0.03	97.57	92.73	47.35
Royalty_YF_3	18,645,743	16,358,356	2.46G	0.03	97.68	92.78	47.34
Flame_ML_1	17,107,950	16,455,822	2.48G	0.03	97.58	92.2	49.1
Flame_ML_2	16,253,678	15,453,856	2.32G	0.03	97.46	92.08	49.25
Flame_ML_3	18,649,538	17,936,747	2.68G	0.03	97.6	92.21	49.12
Flame_YL_1	21,385,428	20,832,609	3.14G	0.03	97.72	92.62	48.25
Flame_YL_2	24,263,706	23,663,852	3.55G	0.03	97.71	92.6	48.24
Flame_YL_3	23,965,176	23,375,864	3.5G	0.03	97.72	92.61	48.26
Flame_MF_1	14,594,251	14,133,498	2.13G	0.03	98	93.24	47.05
Flame_MF_2	15,245,674	14,828,498	2.23G	0.03	97.54	93.18	47.21
Flame_MF_3	17,478,435	16,813,785	2.53G	0.03	98.26	93.36	47.19
Flame_YF_1	9,879,868	9,244,289	1.38G	0.03	96.99	91.67	48.19
Flame_YF_2	9,905,378	9,253,967	1.39G	0.03	96.92	91.64	48.2
Flame_YF_3	10,638,498	9,988,363	1.5G	0.03	96.89	91.61	48.18

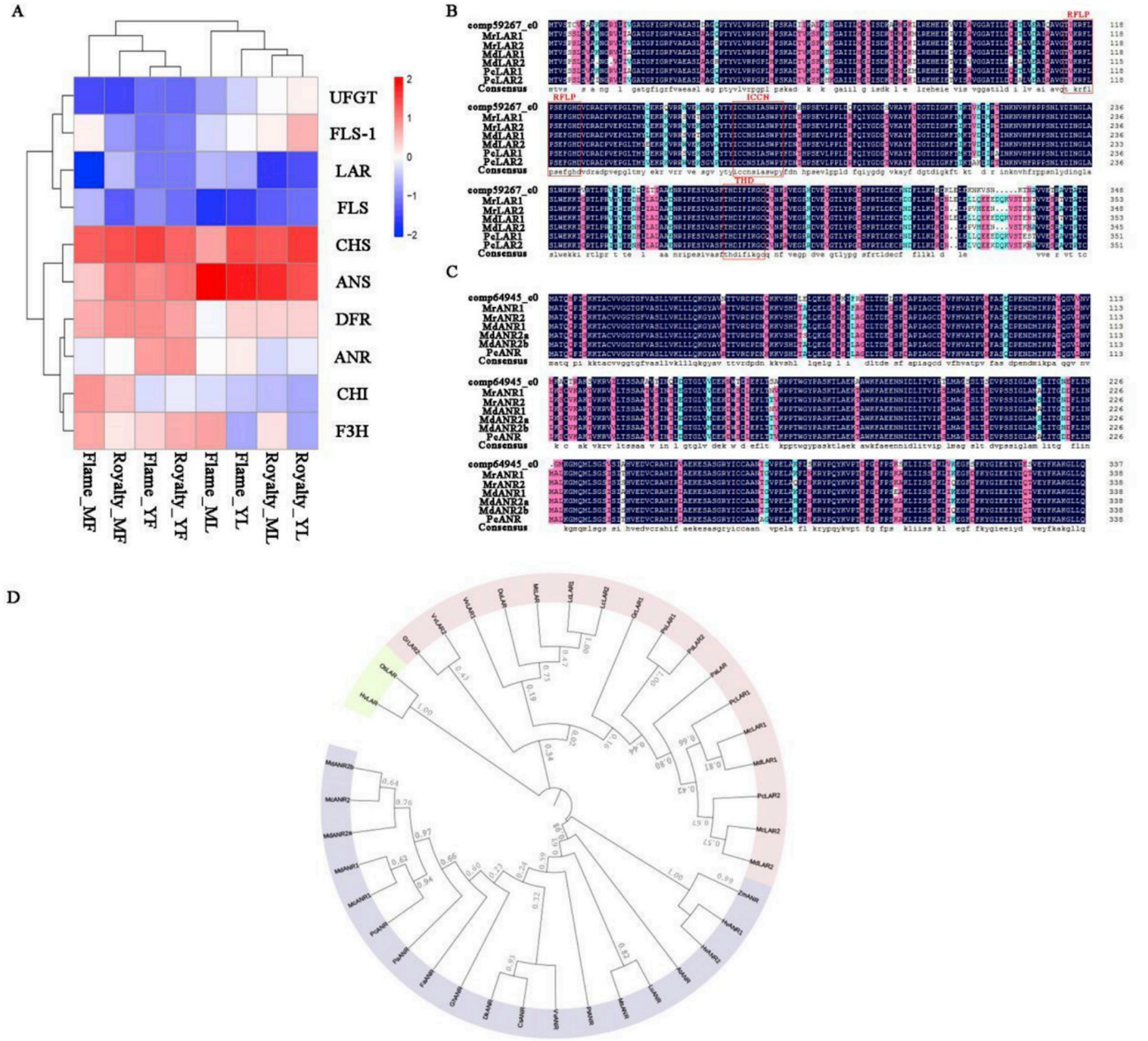

Fig. 1. Bioinformatic analysis of *MrLAR* and *MrANR* in leaves and fruit peels. (A) Transcriptome analysis of developmental stages of *Malus* leaves and fruit peels. Flame_YL and Flame_ML represented the leaves of *Malus* spp. 'Flame' at young and mature stages, respectively. Royalty_YL and Royalty_ML represent the leaves of *Malus* spp. 'Royalty' at the young and mature stage, respectively. Flame_YF and Flame_MF represent the fruit peels of *Malus* spp. 'Flame' at the young and mature stage, respectively. Royalty_YF and Royalty_MF represent the fruit peels of *Malus* spp. 'Royalty' at the young and mature stage, respectively. Unigene IDs are as follows: comp36030_c0, *UFGT*; comp66765_c0, *FLS-1*; comp59267_c0, *LAR*; comp68350_c0, *FLS*; comp72603_c0, *CHS*; comp68723_c0, *ANS*; comp64209_c0, *DFR*; comp64945_c0, *ANR*; comp62471_c0, *CHI*; comp65910_c0, *F3H*. Red and blue colors represent up- and down-regulation, respectively. Heatmap on the left was made using the ggplot2 function in R. (B, C) Alignment of the deduced LAR and ANR amino acid sequences from the two crabapple cultivars and in other plant species. Letters on navy blue background indicates conserved amino acid sequences, similar amino acids are indicated by the red and light blue backgrounds. The RFLP, ICCN, and THD motifs are boxed. (D) Phylogenetic analysis of the *LAR* and *ANR* genes from crabapple plants and other plant species. Phylogenic and molecular evolutionary analysis was conducted using MEGA version 5.1 and ITOL. GenBank database IDs are as follows: *Malus domestica* LAR1, MdLAR1, AFZ93013.1; *Malus domestica* LAR2, MdLAR2, AFZ93011.1; *Vitis vinifera* LAR1, VvLAR1, NP_001267887.1; *Vitis vinifera* LAR2, VvLAR2, NP_001268089.1; *Prunus cerasus* LAR1, PcLAR1, AGG18112.1; *Hordeum vulgare* LAR, HvLAR, CAI56320.1; *Desmodium uncinatum* LAR, DuLAR, CAD79341.1; *Oryza sativa* LAR, OsLAR, XP_015630916.1; *Pisum sativum* LAR, PsLAR, AII26024.1; *Prunus avium* LAR, PaLAR, ADY15310.1; Gossypium raimondii LAR1, GrLAR1, CAI56324.1; Gossypium raimondii LAR2, GrLAR2, CAI56325.1; *Lotus corniculatus* LAR1, LcLAR1, ABC71324.1; *Lotus corniculatus* LAR2, LcLAR2, ABC71330.1; *Medicago truncatula* MtLAR, CAI56327.1; *Malus domestica* ANR1, MdANR1, JN035299; *Malus domestica* ANR2a, MdANR2a, JN035300; *Malus domestica* ANR2b, MdANR2b, JN035301; *Prunus cerasus ANR*, PcANR, DQ251189; *Fragaria ananassa* ANR, FaANR, DQ664192; *Vitis vinifera* ANR, VvANR, XM_002271336; *Populus trichocarpa* ANR, PtANR, XM_002317234; *Gossypium hirsutum* ANR, GhANR, EF187443; *Diospyros kaki* ANR, DkANR, AB195284; *Camellia sinensis* ANR, CsANR, AY641729; *Lotus uliginosus* ANR, LuANR, EF197823; *Medicago sativa* ANR, MsANR, HM754630; *Arabidopsis thaliana* ANR, AtANR, NM_104854; *Hordeum vulgare* ANR1, HvANR1, AK373696; *Hordeum vulgare* ANR2, HvANR2, AK365124; *Zea mays* ANR, ZmANR, BT06443. (For interpretation of the references to color in this figure legend, the reader is referred to the Web version of this article.)

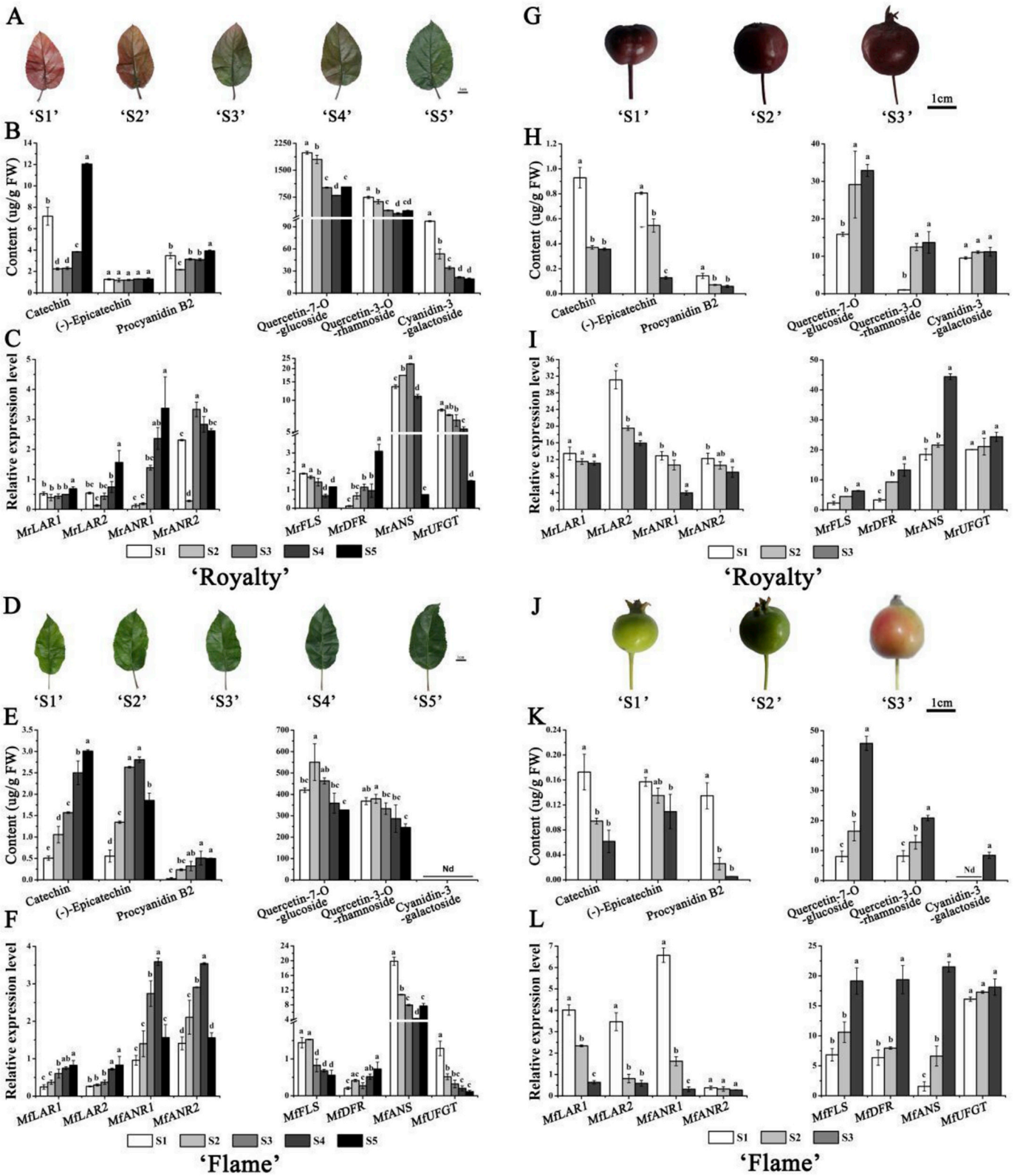

Fig. 2. Phenotypes, flavonoid contents, and expression profiles of flavonoid biosynthesis related genes during late development of leaves and fruit peels of 'Royalty' and 'Flame'. (A, D) Typical phenotypes of 'Royalty' and 'Flame' at five leaf developmental stages. (B, E) The accumulation of major flavonoid compounds in 'Royalty' and 'Flame' at five leaf developmental stages. (C, F) Expression analysis of flavonoid related biosynthetic genes in 'Royalty' and 'Flame' at five leaf developmental stages. (G, J) Typical phenotypes of 'Royalty' and 'Flame' at three fruit peel developmental stages. (H, K) The accumulation of major flavonoid compounds in 'Royalty' and 'Flame' at three fruit peel developmental stages. (I, L) Expression analysis of flavonoid related biosynthetic genes in 'Royalty' and 'Flame' at three fruit peel developmental stages. The 'S' represent 'stage'. Error bars indicate the standard error of the mean ± SE of three replicate measurements. Scale bars = 1 cm. Different letters above the bars indicate significantly different values ($P < 0.05$) calculated using one-way analysis of variance (ANOVA) followed by a Tukey's multiple range test.

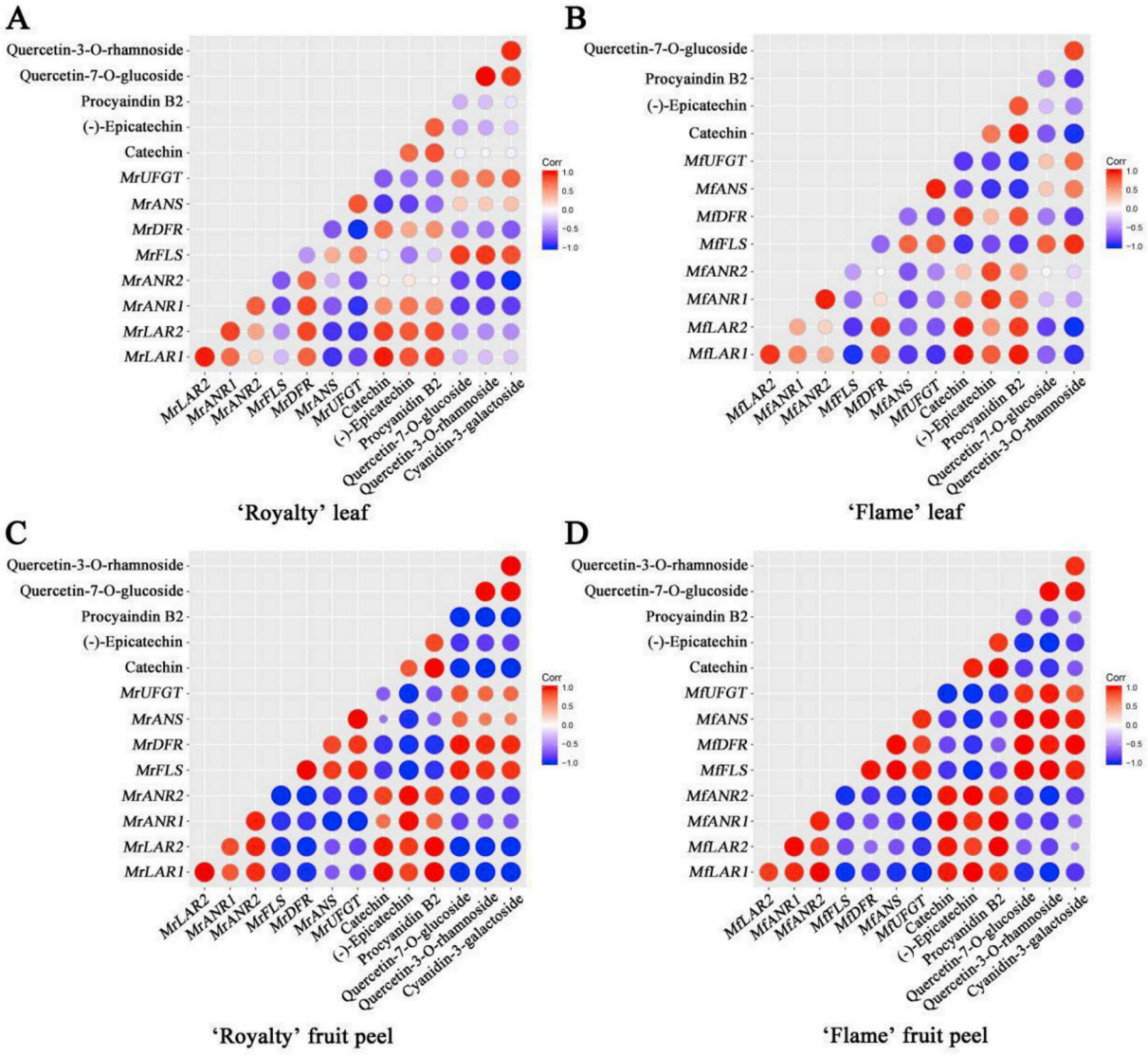

Fig. 3. Heat map showing the correlation between flavonoid compounds and related structural genes in the leaves and fruit peels of 'Royalty' and 'Flame'. (A) Correlation analysis for 'Royalty' leaves. (B) Correlation analysis for 'Flame' leaves. (C) Correlation analysis for 'Royalty' fruit peel. (D) Correlation analysis for 'Flame' fruit peel. Correlation analyses were performed using the cor function in R. Red and blue colors represent increased and decreased expression, respectively. The size of the circle is proportional to the correlation. (For interpretation of the references to color in this figure legend, the reader is referred to the Web version of this article.)

absence of anthocyanin (Fig. 2E). The PA levels were significantly higher in stage S1 than those in S2 and S3 in the fruit peels of both 'Royalty' and 'Flame', while the anthocyanin contents continuously increased with fruit peel development (Fig. 2H and K). The expressions of the quercetin-related *FLS* gene and the anthocyanin biosynthetic genes; *DFR* (dihydroflavonol 4-reductase), *ANS* (anthocyanidin synthase), and *UFGT* (UDP-glucose flavonoid 3-O-glucosyl transferase); decreased with the development of crabapple leaves, while the expression of PA biosynthetic genes increased (Fig. 2C and F). The opposite expression trends of the genes related to quercetin, anthocyanin, and PA were observed in the fruit peels (Fig. 2I, L).

To better understand the effects of the *LAR* and *ANR* genes on the entire flavonoid pathway, we generated a heat map showing the correlations between flavonoid compounds and the relative expression of associated structural genes in the two cultivars (Fig. 3). In 'Royalty' leaves, we observed a higher correlation between *MrLAR1* expression and catechin levels compared to *MrLAR2* and catechin, which was also the case for *MrANR1* expression and epicatechin compared to *MrANR2* and epicatechin. In addition, we also found the high correlation between *LAR1*, *2* expression and epicatechin levels in both leaf and fruit peel of 'Royalty' and 'Flame', consistent with previous reports *Camellia sinensis* (Wang et al., 2018). No obvious differences in relevance between compounds and gene expression patterns in 'Flame' leaves and fruit peels were observed. The correlation between levels of catechin and PAs was higher than between epicatechin and PAs in both leaf and fruit peel. We also observed that the negative correlation between levels of PAs and quercetin (quercetin-7-O-glucoside and quercetin-3-O-rhamnoside) in the leaves of 'Flame' was lower than the correlation between the levels of quercetin (quercetin-7-O-glucoside and quercetin-3-O-rhamnoside), cyanidin-3-galactoside, and PA, in 'Royalty' leaves. The negative correlations between quercetin (quercetin-7-O-glucoside and quercetin-3-O-rhamnoside), cyanidin-3-galactoside, and PAs in the fruit peel of 'Royalty' were lower than the correlations between quercetin (quercetin-7-O-glucoside and quercetin-3-O-rhamnoside), cyanidin-3-galactoside, and PAs in 'Flame' fruit peels. The concentration of quercetin (quercetin-7-O-glucoside and quercetin-3-O-rhamnoside) and cyanidin-3-galactoside gradually decreased during leaf development, while the concentration of PAs gradually increased (Fig. 3 and Table S2).

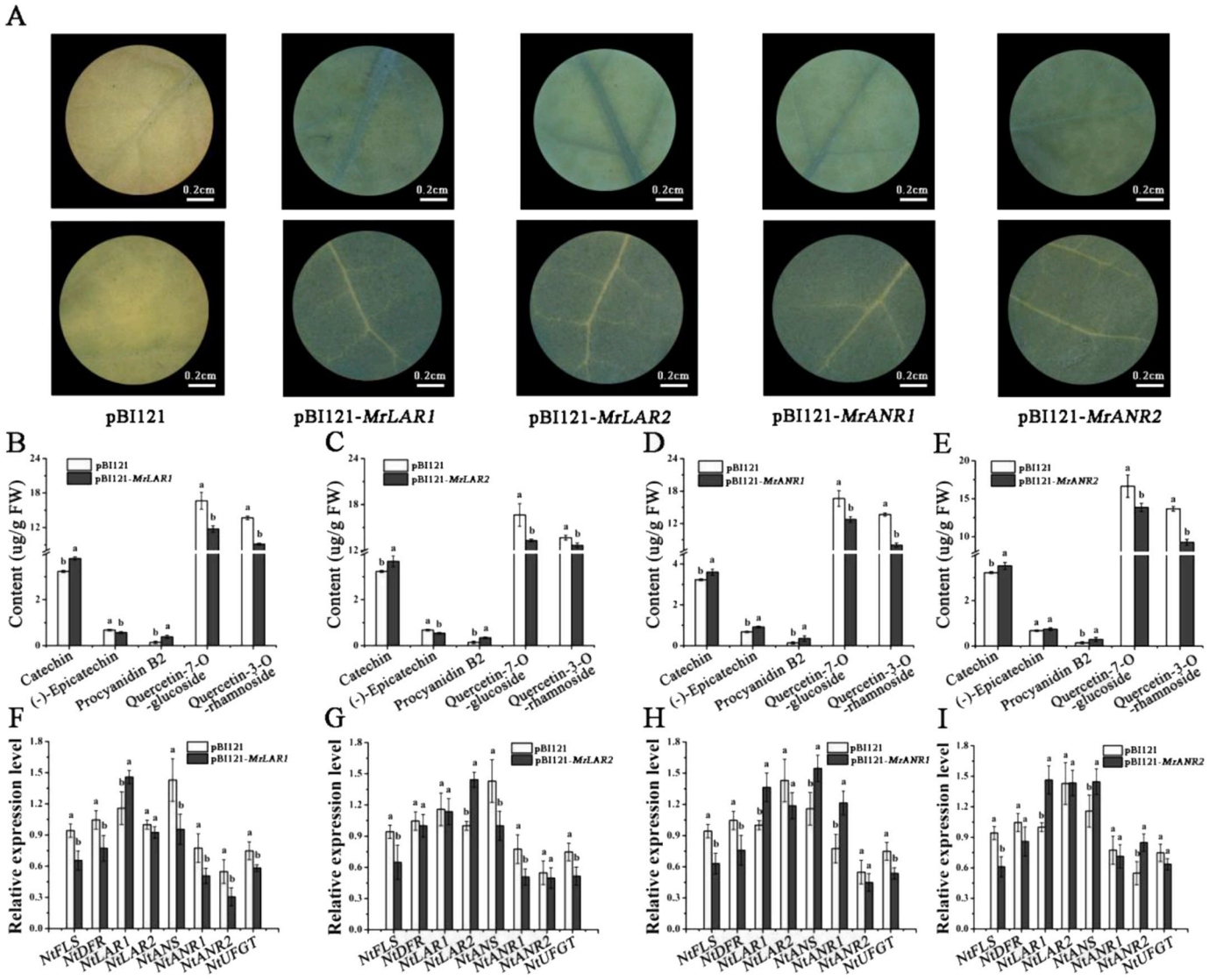

Fig. 4. Ectopic expression of the *MrLAR* and *MrANR* genes in tobacco leaves. (A) 4-Dimethylaminocinnamalde-hyde (DMACA) staining of transgenic tobacco leaves. (B, C, D, E) Concentration of flavonoid compounds in the *MrLAR1*, *2* and *MrANR1*, *2* transgenic tobacco leaves. (F, G, H, I) qRT-PCR analysis of flavonoid pathway related genes in the *MrLAR1*, *2* and *MrANR1*, *2* transgenic tobacco leaves. Error bars indicate the mean ± SE of three replicate reactions. Scale bars = 0.2 cm. Different letters above the bars indicate significantly different values ($P < 0.05$) calculated using one-way analysis of variance (ANOVA) followed by a Tukey's multiple range test.

Taken together these results indicate a role for *LAR* and *ANR* genes in PA accumulation and we identified opposite expression patterns of quercetin, anthocyanin, and PAs in the leaves and fruit peels of crabapples during late development.

3.3. Overexpression of MrLAR1 and 2 and MrANR1 and 2 in tobacco (N. tabacum) plants

To understand the effects of *MrLAR1* and *2* and *MrANR1* and *2*'s ectopic expressions on the whole flavonoid pathway, constructs containing the vectors 35S::*MrLAR* (pBI121, for overexpression) and 35S::*MrANR* (pBI121, for overexpression) were separately agroinfiltrated into tobacco (*N. benthamiana*) plants. Leaf discs containing pBI121-*MrLAR1*, *2* and pBI121-*MrANR1*, 2 had a darker color than the pBI121 empty vector control leaf discs (Fig. 4A). HPLC analysis indicated significantly higher accumulations of catechin and PAs in *MrLAR1* and *2* over-expressing leaves (Fig. 4B and C), and a significantly higher accumulation of catechin, epicatechin and PA in *MrANR1*, *2* over-expressing leaves (Fig. 4D and E). The quercetin contents were significantly lower in *MrLAR1*, *2* and *MrANR1*, *2* over-expressing leaves, while no anthocyanin was detected (Fig. 4).

Gene expression analysis further revealed that the expression levels of the quercetin-related *NtFLS* gene and the anthocyanin-related *NtUFGT* (UDP-glucose flavonoid 3-O-glucosyl transferase) genes were significantly lower in the *MrLAR1* and *2* over-expressing lines compared with the control lines (Fig. 4F and G). Interestingly, over-expression of *MrLAR1* and *2* in tobacco repressed not only the expression of *NtUFGT* and *NtFLS,* but also the expression of the endogenous genes *NtANR1* and *2* (Fig. 4F and G).

Collectively, the expression of *MrLAR* and *MrANR* correlated with PA accumulation, and overexpression of *MrLAR1*, *2* and *MrANR1*, *2* in tobacco promoted the biosynthesis of PA in leaves and inhibited the accumulation of anthocyanin and quercetin.

3.4. Silencing of MrLAR1, 2 and MrANR1, 2 in crabapple

To investigate the functions of *MrLAR* and *MrANR* in crabapple, we suppressed their expression in the leaves of 'Royalty' by TRV-GFP (Tian

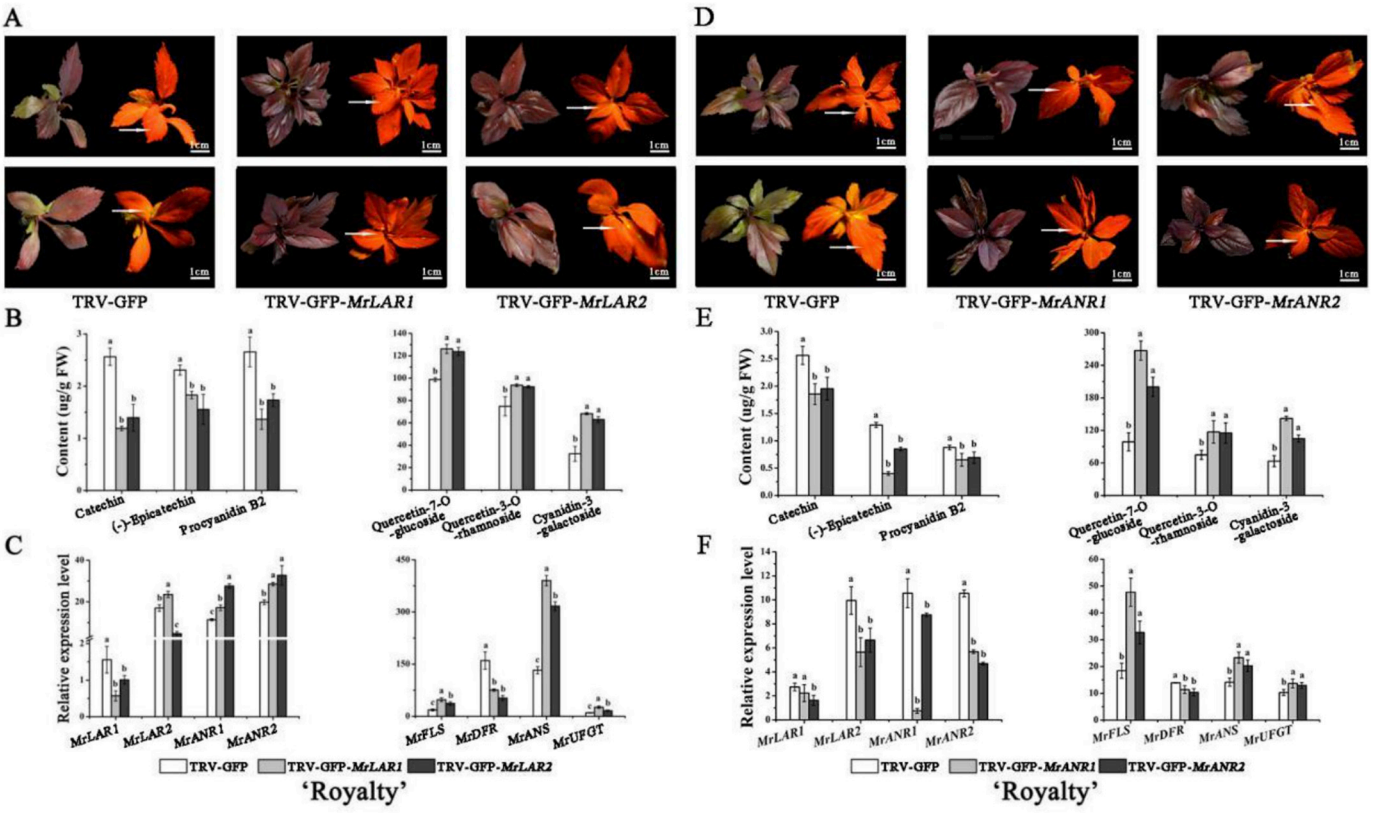

Fig. 5. Silencing of *MrLAR1, 2* and *MrANR1, 2* genes in 'Royalty'. (A, D) Phenotypes were visualized at 14 days post infiltration in 'Royalty'. (B, E) The flavonoid compound concentrations in TRV-GFP-*MrLAR1, 2* and TRV-GFP-*MrANR1, 2* transgenic 'Royalty' plants. (C, F) qRT-PCR analysis of flavonoid pathway related genes in TRV-GFP-*MrLAR1, 2* and TRV-GFP-*MrANR1, 2* transgenic 'Royalty' plants. Error bars indicate the mean ± SE of three replicate reactions. Scale bars = 1 cm. Different letters above the bars indicate significantly different values ($P < 0.05$) calculated using one-way analysis of variance (ANOVA) followed by a Tukey's multiple range test.

et al., 2017). In contrast to the control leaves, green fluorescence was observed under UV light in the petiole and veins of the transgenic seedlings, which indicates that TRV infected crabapple plants successfully (Fig. 5A and D), and a more prominent red leaved phenotype was observed in new buds at 14 days post-infection (dpi) (Fig. 5A and D). HPLC analysis revealed that the levels of quercetin and anthocyanin were higher in *MrLAR1, 2* and *MrANR1, 2* silenced plants compared to control plants, while the catechin, epicatechin, and proanthocyanidin levels were lower (Fig. 5B and E).

Gene expression analysis further revealed a significant increase in the expression of the quercetin related *MrFLS* gene and anthocyanin related *MrUFGT* gene in transgenic leaves (Fig. 5C and F). The expression of the flavonoid related genes *MrFLS, MrANS, MrANR1, MrANR2*, and *MrUFGT* increased in the *MrLAR1, 2* silenced plants compared to control plants of 'Royalty', while the expression of the flavonoid related genes *MrFLS, MrANS,* and *MrUFGT* increased in the *MrANR1, 2* silenced plants compared to controls plants of 'Royalty'. In addition, the gene *MrLAR2* also increased in the *MrLAR1* silenced plants compared to control plants of 'Royalty', and the gene *MrLAR1* and gene *MrLAR2* also weakly increased in the *MrANR1, 2* silenced plants compared to control plants (Fig. 5C and F).

Interestingly, the expression of the PA structural genes, *MrANR1* and *MrANR2*, was significantly higher in *MrLAR1* and *2* transgenic leaves (Fig. 5C), while a significant decrease in epicatechin abundance was observed in silenced *MrLAR1* and *2* lines compared to the control lines (Fig. 5B).

Taken together, silencing *MrLAR1, 2* and *MrANR1, 2* expressions in crabapple promoted the biosynthesis of quercetin and anthocyanin in leaves, but inhibited PA accumulation.

4. Discussion

4.1. Differences in flavonoid contents in different cultivars at different developmental stages

Plants produce flavonoids, such as quercetins, anthocyanins, and PAs, which can accumulate to high levels in seed coat, leaves, flowers, fruits, and bark (Dixon et al., 2005). These flavonoids provide protection against microbial pathogens, pests, and UV radiation, as well as attracting insect pollinators. The levels of flavonoids vary significantly at different developmental stages and between cultivars and areas affected by environment conditions (Shinozaki et al., 2018). Here, we detected significantly lower flavonoid levels, with the exception of epicatechin, in the leaves of 'Flame' compared with those of 'Royalty' during late development (Fig. 2B and E). In the fruit peels, we observed higher levels of catechin and epicatechin in 'Royalty' compared with 'Flame', while the differences in quercetin, anthocyanin, and PA contents were minor during late development (Fig. 2H and K). The flavonoid contents were higher in leaves compared with fruit peels in both cultivars during late development (Fig. 2).

4.2. MrLAR and MrANR genes involved in PA biosynthesis

LAR and ANR enzymes catalyze the conversion of anthocyanin and leucoanthocyanindin (flavan-3,4-diols) to catechin and epicatechin, respectively, and share the same leucoanthocyanidin precursors (Xie et al., 2003; Li et al., 2016). Potential competition between the *LAR* and *ANR* enzymes in apple has been reported, and ectopic expression of *MdLAR* genes in tobacco resulted in decreased expression of *NtANR1* and *NtANR2*, and an increased expression of *NtLAR* (Liao et al., 2015).

In our study, ectopic expression of the *MrLAR1* and *2* in tobacco suppressed expression of *NtANR1* and *2* (Fig. 4F and G), while silencing *MrLAR1* and *2* resulted in a significant increase in *MrANR1* and *2* expressions in 'Royalty' (Fig. 5C). Interestingly, the accumulation of epicatechin significantly decreased in tobacco as a consequence of the over-expression of *MrLAR1* and *2*, while *NtANR1* and *2* expressions decreased (Fig. 5). We noted that a corresponding reduction in epicatechin accumulation following *MrLAR1* and *2* silencing, while the expression of the *MrANR1* and *2* genes increased compared with the TRV-GFP control (Fig. 5C). This is consistent with a recent study showing that ectopic expression of the tea (*Camellia sinensis*) *CsLAR* gene in tobacco results in higher levels of epicatechin than of catechin, suggesting that *LAR* may also be involved in epicatechin biosynthesis (Pang et al., 2013; Liao et al., 2015). Catechin might be formed through chemical epimerization of epicatechin (Xie et al., 2004); however, it has also been reported that ANR proteins from grapevine, tea, and apple have epimerase activity and may have a redundant function in converting anthocyanin to a mixture of epicatechin and catechin (Gargouri et al., 2010; Pang et al., 2013; Li et al., 2016).

It has been reported that over-expression of *ANR* in tobacco results in increased levels of PAs (Xie et al., 2003; Han et al., 2012), while silencing of ANR results in decreased PA levels (Ratanasut et al., 2015). However, over-expression, or loss-of-function, of *LAR* genes also results in an increase in PA in tobacco and a decrease in PA contents in grapevine and apple (Gagné et al., 2009; Han et al., 2012). In our study, over-expression of *MrLAR1*, *2* and *MrANR1*, *2* in tobacco resulted in a significant increase in PA contents (Fig. 4), while we observed lower PA amounts in the silenced *MrLAR1*, *2* and *MrANR1*, *2* lines compared to the controls (Fig. 5).

Taken together, these results indicate competition between the combined effects of *MrLAR1* and *2* versus the combined effects of *MrANR1* and *2*, which prompted us to infer that *MrLAR1* and *2* contribute to epicatechin biosynthesis, and that the complex relationship between catechin and epicatechin remains to be elucidated (For model see Fig. 6). The *MrLAR* and *MrANR* competition and their role in PA biosynthesis in crabapple was consistent with previous studies (Liao et al., 2015).

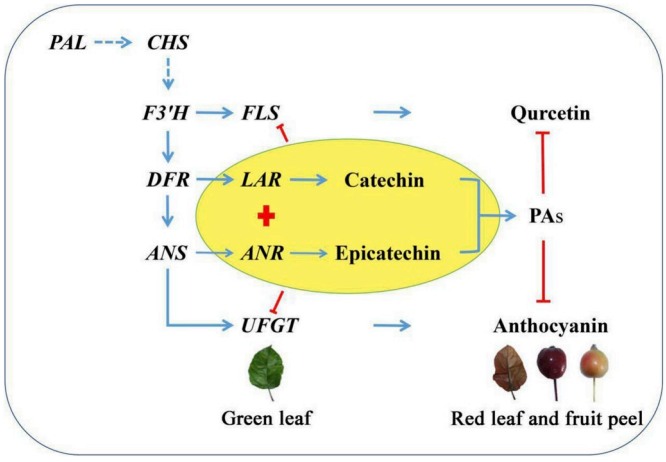

Fig. 6. Model of the mechanism regulating the biosynthesis of PAs, anthocyanin and quercetin in leaves and fruit peels. *LAR* and *ANR* genes are involved in PAs biosynthesis, which competitively inhibits the biosynthesis of anthocyanin and quercetin during the late development of leaf and fruit peel. This competitive inhibition involves not only the inhibition of the structural genes, but also the substrates (PAs, quercetin and anthocyanin) in leaf and fruit peel. In addition, the *LAR1* and *2* genes play a potential assisting role in epicatechin biosynthesis. The blue line and red lines indicate positive and negative effects, respectively. (For interpretation of the references to color in this figure legend, the reader is referred to the Web version of this article.)

4.3. A negative correlation between quercetin, anthocyanin, and PA levels

The biosynthetic pathways leading to anthocyanin and PA share the same anthocyanin precursors, such as leucoanthocyanidins and anthocyanins (Li et al., 2016). Previous studies have shown inverse expression patterns between genes involved in anthocyanin and PA synthesis (Xie et al., 2003; Tian et al., 2017; Li et al., 2016). In our study, we consistently observed a negative correlation between levels of quercetin, anthocyanin, and PAs in crabapple leaves and fruit peels (Fig. 2). We also observed opposite expression trends between the structural genes involved in quercetin, anthocyanin, and PA synthesis (Fig. 2), and documented negative correlations between quercetin, anthocyanin, and PA levels in both cultivars by correlation analysis (Fig. 3). The opposite trends between levels of quercetin, anthocyanin, and PAs were also apparent in the *MrLAR1*, *2* and *MrANR1*, *2* overexpressing tobacco leaves (Fig. 4). Furthermore, the abundance of quercetin and anthocyanin significantly increased in the TRV-GFP-*MrLAR1*, *2* and TRV-GFP-*MrANR1*, *2* lines compared to the TRV-GFP controls (Fig. 5), and the young 'Royalty' leaves had a deeper red color than those of the TRV-GFP control lines (Fig. 5A). These results are consistent the red coloration of leaves being mainly due to the accumulation of flavonoids (anthocyanins) (Tian, 2014). In addition, the expression trends of flavonoid related genes in tobacco and crabapple indicated that *LAR* and *ANR* are the same and are both negatively correlated with *FLS* or *UFGT* (Figs. 4 and 5), which is also consistent with previous reports (Kovinich et al., 2012). The negative correlation between quercetin, anthocyanin, and PAs was much more significant in the fruit peels than in the leaves. In the leaves, the negative correlation was much more significant in the 'Flame' than in 'Royalty', while the opposite trends were observed in Royalty' and 'Flame' fruit peels (Figs. 3 and 6).

5. Conclusions

We observed differences in flavonoid contents in different late developmental stages and cultivars and confirmed that the *LAR* and *ANR* genes are involved in PA biosynthesis by over-expression or silencing *MrLAR1*, *2* and *MrANR1*, *2* in tobacco and crabapple. We conclude that higher PA levels result in repressed anthocyanin and quercetin production. We propose that the *MrLAR* genes may promote the formation of epicatechin, and the *MrANR* gene may also covert anthocyanidin into catechin in the PA biosynthetic pathway. A model summarizing our findings is presented in Fig. 6.

Author contributions

Conceived and designed the experiments: JT YY. Performed the experiments: HL JZ LK. Analyzed the data: JZ JT YY. Contributed reagents/materials/analysis tools: YY TS. Wrote the paper: HL JT YY.

Acknowledgements

We thank the Key Laboratory of New Technology in Agricultural Application of Beijing at the Beijing University of Agriculture and the Beijing Nursery Engineering Research Center for Fruit Crops for providing experimental resources. We also thank PlantScribe (www.plantscribe.com) for editing this manuscript. Financial support was provided by 'National Natural Science Foundation of China' (31772263), 'the Project of Construction of Innovative Teams and the Teacher Career Development for Universities and Colleges Under Beijing Municipality' (IDHT20180509), 'Supporting Plan for Cultivating High Level Teachers in Colleges and Universities in Beijing' (5045243001).

Appendix A. Supplementary data

Supplementary data to this article can be found online at https://doi.org/10.1016/j.plaphy.2019.03.003.

References

Anders, S., Huber, W., 2010. Differential expression analysis for sequence count data. Genome Biol. 11, R106.

Anders, S., Pyl, P.T., Huber, W., 2015. HTSeq-a Python framework to work with high-throughput sequencing data. Bioinformatics 31, 166–169.

Benjamini, Y., Hochberg, Y., 1995. Controlling the false discovery rate: a practical and powerful approach to multiple testing. J. R. Stat. Soc. B. 57, 289–300.

Chevalier, M., Perrochon, E., Barbeau, G., Tellier, M., 2003. Use of dmaca to visualise flavan-3-ols in grape berry skins (*Vitis vinifera* L., cv cabernet franc). J. Int. Sci. Vigne Vin 37, 195–198.

Dixon, R.A., Xie, D.Y., Sharma, S.B., 2005. Proanthocyanidins-a final frontier in flavonoid research? New Phytol. 165, 9–28.

Gagné, S., Lacampagne, S., Claisse, O., Gény, L., 2009. Leucoanthocyanidin reductase and anthocyanidin reductase gene expression and activity in flowers, young berries and skins of *Vitis vinifera* L. spp. Cabernet-Sauvignon during development. Plant Physiol. Biochem. (Montrouge) 47, 282–290.

Gargouri, M., Chaudière, J., Manigand, C., Maugé, C., Bathany, K., Schmitter, J.M., 2010. The epimerase activity of anthocyanidin reductase from *vitis vinifera* and its regiospecific hydride transfers. Biol. Chem. 391, 219–227.

Han, Y., Vimolmangkang, S., Soriaguerra, R.E., Korban, S.S., 2012. Introduction of apple *ANR* genes into tobacco inhibits expression of both *CHI* and *DFR* genes in flowers, leading to loss of anthocyanin. J. Exp. Bot. 63, 2437–2447.

He, X., Zhao, X., Gao, L., Shi, X., Dai, X., Liu, Y., 2018. Isolation and characterization of key genes that promote flavonoid accumulation in purple-leaf tea (*Camellia sinensis* L.). Sci. Rep. 8, 130.

Henrykirk, R.A., Mcghie, T.K., Andre, C.M., Hellens, R.P., Allan, A.C., 2012. Transcriptional analysis of apple fruit proanthocyanidin biosynthesis. J. Exp. Bot. 63, 5437–5450.

Jefferson, R.A., Kvanagh, T.A., Bevan, M.W., 1987. Gus fusions: beta-glucuronidase as a sensitive and versatile gene fusion marker in higher plants. EMBO J. 6, 3901–3907.

Kovinich, N., Saleem, A., Rintoul, T.L., Brown, D.C., Arnason, J.T., Miki, B., 2012. Coloring genetically modified soybean grains with anthocyanins by suppression of the proanthocyanidin genes *ANR1* and *ANR2*. Transgenic Res. 21, 757–771.

Kumar, S., Tamura, K., Nei, M., 2004. MEGA3: integrated software for molecular evolutionary genetics analysis and sequence alignment. Briefings Bioinf. 5, 150–163.

Langmead, B., Trapnell, C., Pop, M., Salzberg, S.L., 2009. Ultrafast and memory-efficient alignment of short DNA sequences to the human genome. Genome Biol. 10, R25.

Li, P., Dong, Q., Ge, S., He, X., Verdier, J., Li, D., 2016. Metabolic engineering of proanthocyanidin production by repressing the isoflavone pathways and redirecting anthocyanidin precursor flux in legume. Plant Biotechnol. J. 14, 1604–1618.

Liao, L., Vimolmangkang, S., Wei, G., Zhou, H., Korban, S.S., Han, Y., 2015. Molecular characterization of genes encoding leucoanthocyanidin reductase involved in proanthocyanidin biosynthesis in apple. Front. Plant Sci. 6, 243.

Livak, K.J., Schmittgen, T.D., 2001. Analysis of relative gene expression data using real-time quantitative PCR and the $2^{-\Delta\Delta CT}$ method. Methods 25, 402–408.

Martin, C., 2013. The interface between plant metabolic engineering and human health. Curr. Opin. Biotechnol. 24, 344–353.

Middleton, E.J., Kandaswami, C., Theoharides, T.C., 2000. The effects of plant flavonoids on mammalian cells: implications for inflammation, heart disease, and cancer. Pharmacol. Rev. 52, 673–751.

Mortazavi, A., Williams, B.A., McCue, K., Schaeffer, L., Wold, B., 2008. Mapping and quantifying mammalian transcriptomes by RNA-Seq. Nat. Methods 5, 621–628.

Pang, Y., Abeysinghe, I.S.B., He, J., He, X.Z., Huhman, D., Mewan, K.M., 2013. Functional characterization of proanthocyanidin pathway enzymes from tea and their application for metabolic engineering. Plant Physiol. 161, 1103–1116.

Ratanasut, K., Monmai, C., Piluk, P., 2015. Transient hairpin RNAi induced silencing in floral tissues of Dendrobium Sonia 'Earsakul' by agroinfiltration for rapid assay of flower colour modification. Plant Cell Tiss. Org. 120, 643–654.

Santos-Buelga, C., Scalbert, A., 2000. Proanthocyanidins and tannin-like compounds-nature, occurrence, dietary intake and effects on nutrition and health. J. Sci. Food Agric. 80, 1094–1117.

Shinozaki, Y., Nicolas, P., Fernandezpozo, N., Ma, Q., Evanich, D.J., Shi, Y., 2018. High-resolution spatiotemporal transcriptome mapping of tomato fruit development and ripening. Nat. Commun. 9, 364.

Tanner, G.J., Francki, K.T., Abrahams, S., Watson, J.M., Larkin, P.J., Ashton, A.R., 2003. Proanthocyanidin biosynthesis in plants. purification of legume leucoanthocyanidin reductase and molecular cloning of its cDNA. J. Biol. Chem. 278, 31647–31656.

Tian, J., Shen, H.X., Zhang, J., Song, T.T., Yao, Y.C., 2011. Characteristics of chalcone synthase promoters from different leaf-color *Malus* crabapple cultivars. Sci. Hortic. 129, 449–458.

Tian, J., 2014. TRV-GFP: a modified Tobacco rattle virus vector for efficient and visualizable analysis of gene function. J. Exp. Bot. 65, 311–322.

Tian, J., Han, Z., Zhang, J., Hu, Y.J., Song, T., Yao, Y., 2015. The balance of expression of dihydroflavonol 4-reductase and flavonol synthase regulates flavonoid biosynthesis and red foliage coloration in crabapples. Sci. Rep. 20, 12228.

Tian, J., Zhang, J., Han, Z., Song, T., Li, J., Wang, Y., Yao, Y.C., 2017. McMYB12 transcription factors co-regulate proanthocyanidin and anthocyanin biosynthesis in *Malus* crabapple. Sci. Rep. 7, 43715.

Trapnell, C., Pachter, L., Salzberg, S.L., 2009. TopHat: discovering splice junctions with RNA-Seq. Bioinformatics 25, 1105–1111.

Velasco, R., Zharkikh, A., Affourtit, J., Dhingra, A., Cestaro, A., Kalyanaraman, A., 2010. The genome of the domesticated apple (*Malus* × *domestica* Borkh.). Nat. Genet. 42, 833–839.

Verdier, J., Zhao, J., Torres-Jerez, I., Ge, S., Liu, C., He, X., 2012. MtPAR MYB transcription factor acts as an on switch for proanthocyanidin biosynthesis in *Medicago truncatula*. Proc. Natl. Acad. Sci. U.S.A. 109, 1766–1771.

Wang, P., Zhang, L., Jiang, X., Dai, X., Xu, L., Li, T., 2018. Evolutionary and functional characterization of leucoanthocyanidin reductases from *Camellia sinensis*. Planta 247, 139–154.

Xie, D.Y., Sharma, S.B., Paiva, N.L., Ferreira, D., Dixon, R.A., 2003. Role of anthocyanidin reductase, encoded by *BANYULS* in plant flavonoid biosynthesis. Science 299, 396–399.

Xie, D.Y., Sharma, S.B., Dixon, R.A., 2004. Anthocyanidin reductases from *Medicago truncatula* and *Arabidopsis thaliana*. Arch. Biochem. Biophys. 422, 91–102.